

A real-space renormalization approach to the Kubo–Greenwood formula in mirror Fibonacci systems

Vicenta Sánchez¹ and Chumin Wang²

¹ Departamento de Física, Facultad de Ciencias, Universidad Nacional Autónoma de México (UNAM), Apartado Postal 70-542, 04510, México DF, Mexico

² Instituto de Investigaciones en Materiales, UNAM, AP 70-360, 04510, DF, Mexico

E-mail: chumin@servidor.unam.mx

Received 2 December 2005, in final form 22 January 2006

Published 7 June 2006

Online at stacks.iop.org/JPhysA/39/8173

Abstract

An exact real-space renormalization method is developed to address the electronic transport in mirror Fibonacci chains at a macroscopic scale by means of the Kubo–Greenwood formula. The results show that the mirror symmetry induces a large number of transparent states in the dc conductivity spectra, contrary to the simple Fibonacci case. A length scaling analysis over ten orders of magnitude reveals the existence of critically localized states and their ac conduction spectra show a highly oscillating behaviour. For multidimensional quasiperiodic systems, a novel renormalization plus convolution method is proposed. This combined renormalization + convolution method has shown an extremely elevated computing efficiency, being able to calculate electrical conductance of a three-dimensional non-crystalline solid with 10^{30} atoms. Finally, the dc and ac conductances of mirror Fibonacci nanowires are also investigated, where a quantized dc-conductance variation with the Fermi energy is found, as observed in gold nanowires.

PACS numbers: 05.10.Cc, 72.15.-v, 71.23.Ft

1. Introduction

In the condensed matter physics, macroscopic crystalline solids are traditionally studied by taking the advantage of the Bloch theorem and the first Brillouin zone [1]. However, these important tools become inadequate or useless when extended defects are introduced, such as in amorphous or quasicrystalline materials, where numerical calculations are usually carried out in clusters with a limited number of atoms [2]. Unfortunately, the long-range aperiodic order and its effects on the transport properties cannot be investigated by using these

numerical results. The real-space renormalization technique, especially the Kadanoff blocking picture [3], has provided a very interesting alternative to address macroscopic quasiperiodic systems. The massive usage of computers in the investigation nowadays has also stimulated its further development. Nevertheless, the traditional real-space renormalization procedures are usually approximate and sometimes give very poor results [4]. In this context, we have recently developed a new renormalization method to calculate the electrical conductivity of Fibonacci systems by iterating directly the Kubo–Greenwood formula [5]. This method does not introduce any additional approximations and is very efficient to be able to address truly macroscopic systems, where quadruple numerical precision should be used. In this paper, we extend this renormalization method to the mirror Fibonacci lattices and analyse the dc and ac electrical conductance of three-dimensional macroscopic systems. Section 2 introduces the mirror Fibonacci lattices and its renormalization procedure, whose detailed formulation is given in the appendix. In section 3, multidimensional systems are studied by using the renormalization + convolution (R + C) method, which is illustrated by using the density of states (DOS) or the eigenvalues of the perpendicular subsystem with respect to the applied electric field. Finally, some conclusive remarks are provided in section 4.

2. Mirror Fibonacci lattices

A Fibonacci chain (FC) can be constructed by using a unique type of atom and alternating two sorts of bonds, A and B , following the Fibonacci sequence. This bond Fibonacci sequence (F_n) is defined as $F_1 = A$, $F_2 = AB$ and $F_n = F_{n-1} \oplus F_{n-2}$, where n is the number of generation. For example, $F_4 = ABAAB$. A mirror Fibonacci sequence (M_n) can be obtained just by connecting a FC to its mirror image, i.e. for instance $M_4 = BAABA-ABAAB$. In order to isolate the quasicrystalline effects, we consider a simple s -band tight-binding Hamiltonian with null self-energies,

$$H = \sum_j \{t_{j,j+1}|j\rangle\langle j+1| + t_{j-1,j}|j\rangle\langle j-1|\}, \quad (1)$$

$t_{ij} = t_A$ or t_B being the hopping integral between nearest-neighbour atoms i and j . For the sake of simplicity, a uniform bond length (a) is taken. There are several manners to examine the electronic localization and transport in solids [6]. In this study, the dc and ac electrical conductivities (σ) are calculated by means of the Kubo–Greenwood formula, which can be written as [7, 8]

$$\sigma_{xx}(\mu, \omega, T) = \frac{e^2 \hbar}{2\pi m^2 \Omega} \int_{-\infty}^{\infty} dE \frac{f(E + \hbar\omega) - f(E)}{\hbar\omega} \text{Tr}[p_x \tilde{G}(E + \hbar\omega) p_x \tilde{G}(E)], \quad (2)$$

where Ω is the system volume and $f(E) = \{1 + \exp[(E - \mu)/k_B T]\}^{-1}$ is the Fermi–Dirac distribution with the Fermi energy μ and the temperature T . The projection of the momentum operator along the applied electrical field is given by $p_x = (im/\hbar)[H, x]$ and using equation (1) we obtain

$$p_x = \frac{ima}{\hbar} \sum_j \{t_{j,j+1}|j\rangle\langle j+1| - t_{j-1,j}|j\rangle\langle j-1|\}. \quad (3)$$

The discontinuity of Green's functions is defined as $\tilde{G}(E) \equiv G^+(E) - G^-(E)$, where $G^+(E)$ and $G^-(E)$ are respectively the retarded and advanced one-particle Green's functions [7].

A smart way to evaluate the Kubo–Greenwood formula in large aperiodic systems is through a real-space renormalization approach [9]. In figure 1, this renormalization procedure is schematically illustrated for the bond Fibonacci case, where the numbers on the left side indicate the generation. The atoms are symbolized by open circles, specifying

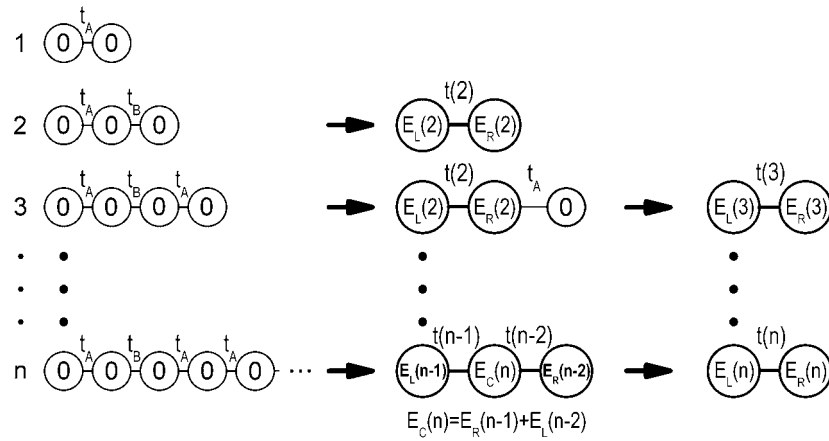


Figure 1. Schematic representation of the renormalization procedure for a FC with bond disorder. The numbers on the left-hand side indicate the generation. Self-energies and hopping strengths are, respectively, specified inside and between the atoms (open circles).

their self-energies and hopping strengths inside and between them, respectively. At end of the renormalization procedure, one gets two effective atoms (larger circles) connected by an effective bond. There is a middle step, in which renormalized chains of lower generation are connected through a common effective atom whose self-energy is given by $E_c(n) = E_R(n-1) + E_L(n-2)$, unlike to the mixing case where lower generation chains are connected together by a hopping t_{AB} [5]. The detailed recursion formulae of the Kubo–Greenwood formula in mirror Fibonacci chains (MFC) are given in the appendix. These formulae were used in the numerical calculation of the results presented in the following section.

For multidimensional quasiperiodic systems, the convolution theorem is used when the Hamiltonian of the system is separable, i.e. $H = H_{\parallel} \otimes I_{\perp} + I_{\parallel} \otimes H_{\perp}$, H_{\parallel} (I_{\parallel}) and H_{\perp} (I_{\perp}) respectively being the Hamiltonian (the identity of the corresponding Hilbert space) of the parallel and perpendicular subsystems with respect to the applied electric field [10]. For instance, the decagonal quasicrystals [2] can be visualized as a periodic stacking of quasiperiodic layers and their Hamiltonian can be expressed as a sum of the periodic and quasiperiodic parts within the nearest-neighbour tight-binding approximation. Therefore, the electrical conductivity can be expressed as [9]

$$\sigma_{xx}(\mu, \omega, T) = \frac{1}{\Omega_{\perp}} \int_{-\infty}^{\infty} dy \sigma_{xx}^{\parallel}(\mu - y, \omega, T) \text{DOS}^{\perp}(y), \quad (4)$$

or

$$\sigma_{xx}(\mu, \omega, T) = \frac{1}{\Omega_{\perp}} \sum_{\beta} \sigma_{xx}^{\parallel}(\mu - E_{\beta}, \omega, T), \quad (5)$$

where σ^{\parallel} is the electrical conductivity of the parallel subsystem; Ω_{\perp} , DOS^{\perp} and E_{β} are respectively the volume, the density of states and the eigenvalues of the perpendicular subsystem, i.e. $H_{\perp}|\beta\rangle = E_{\beta}|\beta\rangle$. In figure 2, the computing times spent through direct calculation of Green's function (open squares) and by using only the convolution technique (open triangles) are compared with those obtained by means of the (R + C) method (open circles). In all these calculations, square lattices with a fixed width of six atoms are used and the numerical computations were performed on a Silicon Graphics O2 workstation with

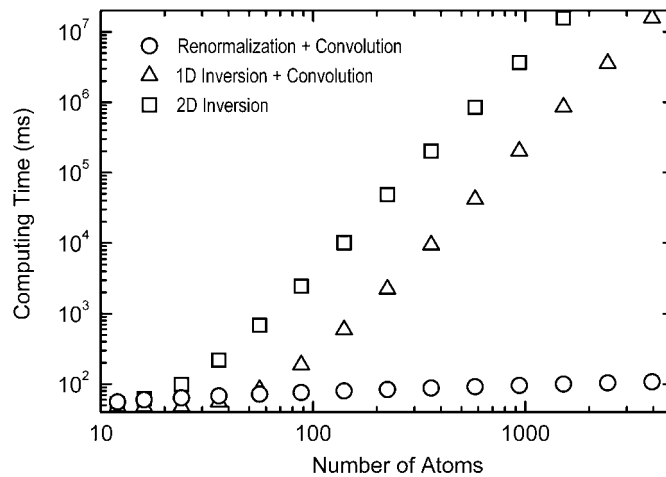


Figure 2. The Kubo–Greenwood formula computing time versus the number of atoms in two-dimensional (2D) square lattices with a fixed width of six atoms, by using the renormalization + convolution method (open circles), one-dimensional (1D) inversion of the Hamiltonian plus convolution (open triangles) and direct 2D inversion (open squares).

a MIPS R12000 microprocessor. It would be worth mentioning that the results obtained from these three approaches are exactly the same. Hence, in the rest of this paper only R + C results will be shown.

3. Results

In figures 3(a) and (b), dc electrical conductivities at zero temperature, $\sigma(\mu, 0, 0) = \sigma_{xx}(\mu, 0, 0)$, are respectively plotted as a function of the Fermi energy (μ) for a FC of 433 494 438 atoms, corresponding to generation $n = 42$, and for a MFC of 866 988 875 atoms, which are connected to two semi-infinite periodic linear chains (leads) with hopping integrals t and null on-site energies. These two quasiperiodic chains have the same Hamiltonian parameters, $t_A = 0.97t$ and $t_B = t$. The imaginary part of the energy in Green's function is $\eta = 10^{-17}t$ and $\sigma_P = (N - 1)e^2a/(\pi\hbar)$ is the dc conductivity of a periodic chain with N atoms. The magnifications around $\mu = 0$ of figures 3(a) and (b) are respectively illustrated in figures 3(a') and (b'). Observe the transparent states located at $\mu = 0$ in both FC and MFC, where this transparency has been analytically demonstrated for the former case in [9]. Additionally, there are many other transparent states in the MFC, as observed in a light propagation study [11]. This appearance of additional transparent states due to the global mirror symmetry of the system has been predicted by an analytical study [12]; similar to those observed in a random symmetric-dimer model [13].

In figures 4(a) and (b), the dependence of σ on the system length is analysed for the states located at $\mu = 0$ and $\mu = 0.729\,373|t|$, respectively, for the same FC (solid circles) and MFC (open circles) as in figure 3. Note that the first state at $\mu = 0$ is a transparent state for every generation of MFC, instead of each six generations for the analysed FC case. It would be worth mentioning that this occurs in each three generations if the FC is built by starting from $F_2 = BA$. Another analysed state ($\mu = 0.729\,373|t|$) is located at the edge of the largest energy gap of the DOS for both FC and MFC. This state shows an oscillating behaviour when the system length increases, revealing a critical localization nature [2].

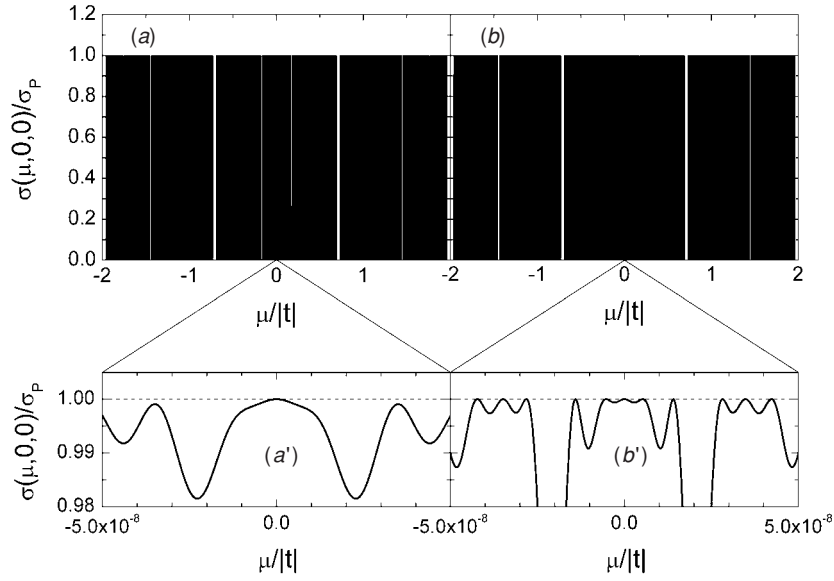


Figure 3. The dc electrical conductivities (σ) of (a) a FC with 433 494 438 atoms and (b) a MFC with 866 988 875 atoms. Magnifications of figures 3(a) and (b) around $\mu = 0$ are, respectively, shown in figures 3(a') and (b').

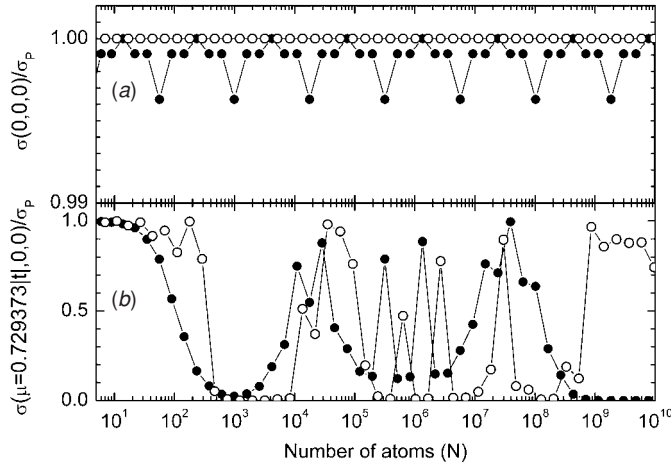


Figure 4. The dc electrical conductivity (σ) versus the number of atoms contained in the same FC (solid circles) and MFC (open circles) as in figure 3, except for the system length.

Continuing with the same systems of figure 3, the dependence of σ on the frequency of the applied electric field is shown in figures 5(a) and (b) for the same states analysed in figures 4(a) and (b), respectively. The solid line represents the analytical solution obtained from a periodic chain of N atoms, which is given by [9]

$$\sigma_{xx}(\mu, \omega, 0) = \frac{8e^2 t^2 a}{\pi(N-1)\hbar^3 \omega^2} \left[1 - \left(\frac{\mu}{2t} \right)^2 \right] \left\{ 1 - \cos \left[(N-1) \frac{\hbar\omega/(2t)}{\sqrt{1 - [\mu/(2t)]^2}} \right] \right\}, \quad (6)$$

for $|\mu| \leq 2|t|$. Note that the transparent states have an ac behaviour very close to the periodic case, contrary to a critically localized state, since the ac conductivity involves states within an

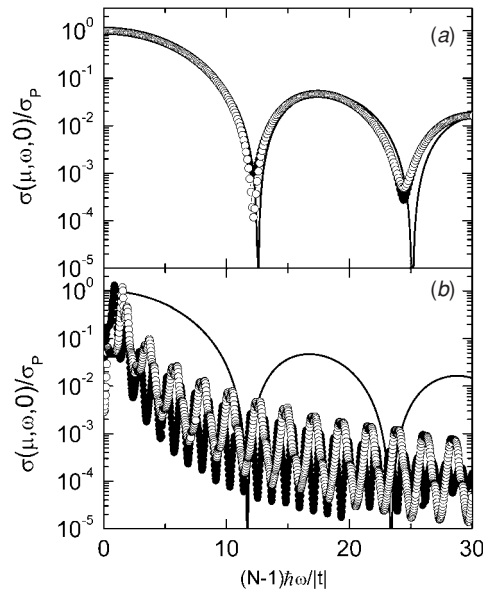


Figure 5. The ac electrical conductivity versus the frequency of the applied electric field for the same FC (solid circles) and MFC (open circles) as in figure 4, evaluated at (a) $\mu = 0$ and (b) $\mu = 0.729373|t|$. The solid line indicates the behaviour of a periodic system.

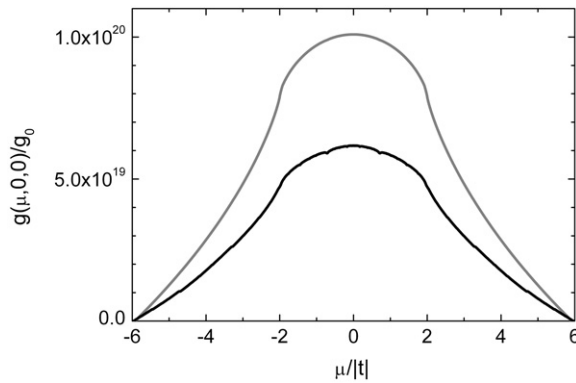


Figure 6. The dc electrical conductance of a 3D solid containing about 1.595×10^{31} atoms when the electric field is applied along a periodic direction (grey line) or along a quasiperiodic direction (black line). The quasiperiodic arrangement has the same system parameters as in figure 3.

interval of $\hbar\omega$ around the Fermi energy (see equation (2)). In most cases, the MFC has larger ac conductivity than that of FC.

For three-dimensional (3D) systems, the electrical conductance (g) can be defined as

$$g(\mu, \omega, T) = \frac{\sigma(\mu, \omega, T)\Omega_{\perp}}{\Omega_{\parallel}}, \quad (7)$$

where Ω_{\perp} and Ω_{\parallel} are the volume in the perpendicular and parallel subspace of the system, respectively. In figure 6, the dc electrical conductance of a 3D solid with 25 172 538 051 atoms in each direction, corresponding to a MFC of generation $n = 49$, is shown when the electric field is applied along a periodic direction (grey line) or a quasiperiodic one (black

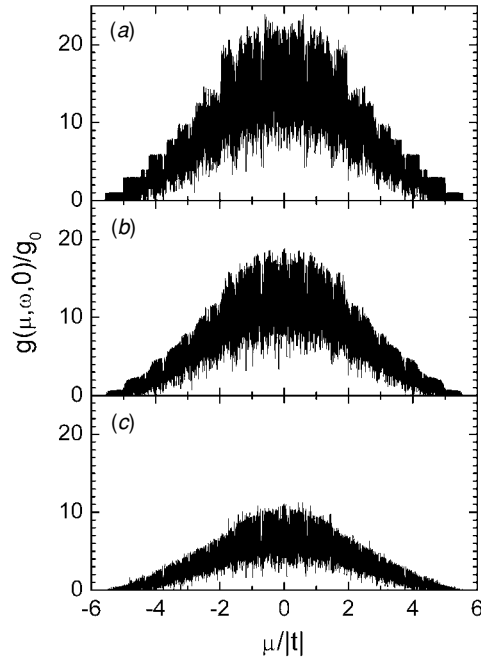


Figure 7. The ac electrical conductance of a nanowire containing $866\,988\,875 \times 6 \times 6$ atoms for (a) $\hbar\omega = 0$, (b) $\hbar\omega = 2|t|/(N_{\parallel}-1)$ and (c) $\hbar\omega = 5|t|/(N_{\parallel}-1)$. The atoms of this nanowire are quasiperiodic arranged on the longer side with the same system parameters as in figure 3, and periodically arranged in the square cross section.

line). The quasiperiodic arrangement has the same system parameters as in figure 3 and the conductance unit is given by $g_0 = 2e^2/h$. The numerical results are obtained by using the convolution equation (4). Observe that a 3% disorder in the hopping strength could cause a 3D electrical conductance that is one order of magnitude smaller than the periodic one. Also, we found that these two spectra are not sensitive to the atomic arrangement in the perpendicular subspace.

In figures 7(a), (b) and (c), the ac electrical conductance of a nanowire is shown for $\hbar\omega = 0$, $2|t|/(N_{\parallel}-1)$ and $5|t|/(N_{\parallel}-1)$, respectively. This nanowire has $N_{\parallel} = 866\,988\,875$ quasiperiodically arranged atoms along the applied electric field and a square cross section of 6×6 periodically arranged atoms. The mirror Fibonacci arrangement in the parallel direction has the same system parameters as in figure 3 and the numerical results are obtained by means of equation (5). The quantized step behaviour of g is still notable in figure 7(a) and it becomes perfect quantum steps if the atoms are periodically arranged along the electric field direction, as found in [9]. This quantized conductance behaviour has been experimentally observed in gold nanowires [14]. However, it can be quickly destroyed when an oscillating electric field is introduced, as shown in figures 7(b) and (c).

4. Conclusions

The real-space renormalization method seems to be very powerful tool to address macroscopic aperiodic systems. Furthermore, combination of the real-space renormalization method with the convolution technique could be an interesting approach to the multidimensional non-crystalline solids. In this paper, we have extended the renormalization method to the MFC and

the results show the existence of a large number of transparent states, instead of a single one in FC. These transparent states could be very important in the behaviour of a low-dimensional solid, since they lead to a ballistic conduction, i.e. the electrons can go from one end to the other without being scattered, giving rise to the phenomenon that the system resistance could be independent of its length.

Acknowledgments

This work has been partially supported by CONACyT-49291, UNAM-IN110305 and IN114805. Computations were performed at Bakliz of DGSCA, UNAM.

Appendix: Renormalization formulae for mirror Fibonacci chains

In this appendix, the renormalization formulae are given for a mirror Fibonacci chain (MFC) with bond disorder. The trace in the Kubo–Greenwood formula (equation (2)) can be written as

$$\text{Tr}[p_x \tilde{G}(E + \hbar\omega) p_x \tilde{G}(E)] = S(E_\omega^+, E^+, n) - S(E_\omega^+, E^-, n) \\ - S(E_\omega^-, E^+, n) + S(E_\omega^-, E^-, n),$$

where $E^\pm = E \pm i\eta$, $E_\omega^\pm = E + \hbar\omega \pm i\eta$ with $\eta \rightarrow 0^+$, and partial sums

$$S(E_\omega^\nu, E^\kappa, n) = \sum_{j,k=1}^{N(n)-1} t_{j,j+1} t_{k,k+1} [2G_{j+1,k}(E_\omega^\nu) G_{k+1,j}(E^\kappa) - G_{j+1,k+1}(E_\omega^\nu) G_{k,j}(E^\kappa) \\ - G_{j,k}(E_\omega^\nu) G_{k+1,j+1}(E^\kappa)],$$

ν and κ being either + or -. These partial sums can be expressed in terms of Green's functions evaluated at the extreme sites of the MFC as

$$S(E_\omega^\nu, E^\kappa, n) = A(E_\omega^\nu, E^\kappa, n) G_{L,L}(E_\omega^\nu) G_{L,L}(E^\kappa) - A(E_\omega^\nu, E^\kappa, n) G_{L,R}(E_\omega^\nu) G_{L,R}(E^\kappa) \\ + B(E_\omega^\nu, E^\kappa, n) G_{L,L}(E_\omega^\nu) G_{L,R}(E^\kappa) + B(E^\kappa, E_\omega^\nu, n) G_{L,R}(E_\omega^\nu) G_{L,L}(E^\kappa) \\ + C(E_\omega^\nu, E^\kappa, n) G_{L,L}(E_\omega^\nu) + C(E^\kappa, E_\omega^\nu, n) G_{L,L}(E^\kappa) \\ + D(E_\omega^\nu, E^\kappa, n) G_{L,R}(E_\omega^\nu) + D(E^\kappa, E_\omega^\nu, n) G_{L,R}(E^\kappa) + F(E_\omega^\nu, E^\kappa, n), \quad (\text{A.1})$$

where the subindices L and R denote the left- and right-end atoms, respectively. The coefficients $A(E_1, E_2, n)$, $B(E_1, E_2, n)$, \dots , $F(E_1, E_2, n)$ in equation (A.1), E_1 and E_2 being either E_ω^ν or E^κ , can be iteratively obtained from quantities of generations $n-1$ and $n-2$, as given in the following:

$$A(E_1, E_2, n) = -[B_0(E_1, E_2, n) + 2\theta_1(E_2, n)A_0(E_1, E_2, n)]^2 \\ - [B_0(E_1, E_2, n) - 2\theta_1(E_1, n)A_0(E_2, E_1, n)]^2,$$

$$B(E_1, E_2, n) = -4\theta_1(E_1, n)A_0(E_2, E_1, n)[B_0(E_1, E_2, n) - \theta_1(E_1, n)A_0(E_2, E_1, n)] \\ - 4\theta_1(E_2, n)A_0(E_1, E_2, n)[B_0(E_1, E_2, n) + \theta_1(E_2, n)A_0(E_1, E_2, n)],$$

$$C(E_1, E_2, n) = 2[-\theta_0(E_2, n)A_0^2(E_1, E_2, n) + \theta_1(E_1, n)K(E_1, E_2, n) \\ + 2\theta_1^2(E_1, n)L(E_1, E_2, n) + J(E_1, E_2, n)],$$

$$D(E_1, E_2, n) = 2[\theta_0(E_2, n)A_0^2(E_1, E_2, n) + \theta_1(E_1, n)K(E_1, E_2, n) \\ + 2\theta_1^2(E_1, n)L(E_1, E_2, n)],$$

and

$$F(E_1, E_2, n) = 2[\theta_0(E_1, n)L(E_1, E_2, n) + \theta_0(E_2, n)L(E_2, E_1, n) + Z(E_1, E_2, n)],$$

where

$$J(E_1, E_2, n) = \theta_3^2(E_1, n)[L(E_1, E_2, n-1) + J(E_1, E_2, n-2)] + \theta_3(E_1, n)K(E_1, E_2, n-1) \\ + J(E_1, E_2, n-1) - \theta_2(E_2, n)[\theta_3(E_1, n)C_0(E_1, E_2, n) + A_0(E_1, E_2, n-1)]^2,$$

$$K(E_1, E_2, n) = 2\theta_3(E_1, n)\theta_4(E_1, n)[L(E_1, E_2, n-1) + J(E_1, E_2, n-2)] \\ + \theta_3(E_1, n)K(E_1, E_2, n-2) - 2\theta_2(E_2, n)[\theta_4(E_1, n)C_0(E_1, E_2, n) \\ - A_0(E_2, E_1, n-2)][\theta_3(E_1, n)C_0(E_1, E_2, n) + A_0(E_1, E_2, n-1)] \\ + \theta_4(E_1, n)K(E_1, E_2, n-1),$$

$$L(E_1, E_2, n) = \theta_4^2(E_1, n)[L(E_1, E_2, n-1) + J(E_1, E_2, n-2)] + \theta_4(E_1, n)K(E_1, E_2, n-2) \\ + L(E_1, E_2, n-2) - \theta_2(E_2, n)[\theta_4(E_1, n)C_0(E_1, E_2, n) - A_0(E_2, E_1, n-2)]^2,$$

$$Z(E_1, E_2, n) = -\theta_2(E_1, n)\theta_2(E_2, n)C_0^2(E_1, E_2, n) + \theta_2(E_1, n)[L(E_1, E_2, n-1) \\ + J(E_1, E_2, n-2)] + \theta_2(E_2, n)[L(E_2, E_1, n-1) + J(E_2, E_1, n-2)] \\ + Z(E_1, E_2, n-1) + Z(E_1, E_2, n-2),$$

$$A_0(E_1, E_2, n) = C_c(E_1, E_2, n) - D_c(E_2, E_1, n),$$

$$B_0(E_1, E_2, n) = A_c(E_1, E_2, n) - A_c(E_2, E_1, n),$$

$$C_0(E_1, E_2, n) = B_0(E_1, E_2, n-2) + B_c(E_1, E_2, n-1) - B_c(E_2, E_1, n-1),$$

$$A_c(E_1, E_2, n) = A_c(E_1, E_2, n-1) + \theta_3(E_1, n)\theta_3(E_2, n)[A_c(E_1, E_2, n-2) \\ + B_c(E_1, E_2, n-1)] + \theta_3(E_2, n)C_c(E_1, E_2, n-1) \\ + \theta_3(E_1, n)D_c(E_1, E_2, n-1),$$

$$B_c(E_1, E_2, n) = B_c(E_1, E_2, n-2) + \theta_4(E_1, n)\theta_4(E_2, n)[A_c(E_1, E_2, n-2) \\ + B_c(E_1, E_2, n-1)] + \theta_4(E_1, n)C_c(E_1, E_2, n-2) \\ + \theta_4(E_2, n)D_c(E_1, E_2, n-2),$$

$$C_c(E_1, E_2, n) = \theta_3(E_1, n)\theta_4(E_2, n)[A_c(E_1, E_2, n-2) + B_c(E_1, E_2, n-1)] \\ + \theta_3(E_1, n)C_c(E_1, E_2, n-2) + \theta_4(E_2, n)C_c(E_1, E_2, n-1),$$

$$D_c(E_1, E_2, n) = \theta_3(E_2, n)\theta_4(E_1, n)[A_c(E_1, E_2, n-2) + B_c(E_1, E_2, n-1)] \\ + \theta_3(E_2, n)D_c(E_1, E_2, n-2) + \theta_4(E_1, n)D_c(E_1, E_2, n-1),$$

$$\theta_0(E, n) = [E - 2E_R(E, n)]^{-1}, \quad \theta_1(E, n) = t(E, n)\theta_3(E, n),$$

$$\theta_2(E, n) = [E - E_R(E, n-1) - E_L(E, n-2)]^{-1},$$

$$\theta_3(E, n) = t(E, n-1)\theta_2(E, n), \quad \text{and} \quad \theta_4(E, n) = t(E, n-2)\theta_2(E, n),$$

E being either E_1 or E_2 . The effective hopping integral $[t(E, n)]$, the effective self-energies of the left $[E_L(E, n)]$ and right $[E_R(E, n)]$ extreme sites are respectively given by

$$t(E, n) = t(E, n-1)t(E, n-2)\theta_2(E, n),$$

$$E_L(E, n) = E_L(E, n-1) + t^2(E, n-1)\theta_2(E, n),$$

and

$$E_R(E, n) = E_R(E, n - 2) + t^2(E, n - 2)\theta_2(E, n).$$

When the system is connected to two semi-infinite periodic leads with hopping integrals t and null on-site energies, Green's functions in equation (A.1) can be written as

$$G_{L,L}(E) = \left\{ E - E_P(E) - E_L(E, n) - t^2(E, n)\theta_0(E, n) - \frac{t^4(E, n)\theta_0^2(E, n)}{E - E_P(E) - E_L(E, n) - t^2(E, n)\theta_0(E, n)} \right\}^{-1}$$

and

$$G_{L,R}(E) = G_{L,L}(E)t^2(E, n)\theta_0(E, n)[E - E_P(E) - E_L(E, n) - t^2(E, n)\theta_0(E, n)]^{-1},$$

where $E_P(E) = (E - i \times \text{sign}[\text{Im}(E)] \times \sqrt{4t^2 - E^2})/2$.

Finally, the initial conditions for the iterative procedure are

$$t(E, 1) = t_A, \quad E_L(E, 1) = E_R(E, 1) = 0, \quad t(E, 2) = t_A t_B / E, \\ E_L(E, 2) = t_A^2 / E, \quad E_R(E, 2) = t_B^2 / E,$$

$$J(E_1, E_2, 1) = K(E_1, E_2, 1) = L(E_1, E_2, 1) = Z(E_1, E_2, 1) = 0, \\ J(E_1, E_2, 2) = -t(E_2, 2)t_A/t_B,$$

$$K(E_1, E_2, 2) = 2t(E_2, 2), \quad L(E_1, E_2, 2) = -t(E_2, 2)t_B/t_A, \quad Z(E_1, E_2, 2) = 0,$$

$$A_c(E_1, E_2, 1) = B_c(E_1, E_2, 1) = C_c(E_1, E_2, 1) = 0, \quad D_c(E_1, E_2, 1) = t_A,$$

$$A_c(E_1, E_2, 2) = t_A^2 / E_1, \quad B_c(E_1, E_2, 2) = t_B^2 / E_2,$$

$$C_c(E_1, E_2, 2) = 0, \quad \text{and} \quad D_c(E_1, E_2, 2) = t_A t_B / E_1 + t_A t_B / E_2.$$

This renormalization method is recommended to use quadruple precision for the numerical evaluations.

References

- [1] Kittel C 1996 *Introduction to Solid State Physics* 7th edn (New York: Wiley)
- [2] Janot C 1994 *Quasicrystals: A Primer* 2nd edn (Oxford: Oxford University Press)
- [3] Stanley H E 1999 Scaling, universality, and renormalization: three pillars of modern critical phenomena *Rev. Mod. Phys.* **71** S358–66
- [4] White S R and Noack R M 1992 Real-space quantum renormalization groups *Phys. Rev. Lett.* **68** 3487–90
- [5] Sánchez V, Pérez L A, Oviedo-Roa R and Wang C 2001 Renormalization approach to the Kubo formula in Fibonacci systems *Phys. Rev. B* **64** 174205
- [6] Oviedo-Roa R, Pérez L A and Wang C 2000 Ac conductivity of the transparent states in Fibonacci chains *Phys. Rev. B* **62** 13805–8
- [7] Economou E N 1983 *Green's Functions in Quantum Physics* 2nd edn (Berlin: Springer) p 156
- [8] Crepieux A and Bruno P 2001 Theory of the anomalous Hall effect from the Kubo formula and the Dirac equation *Phys. Rev. B* **64** 014416
- [9] Sánchez V and Wang C 2004 Application of renormalization and convolution methods to the Kubo–Greenwood formula in multidimensional Fibonacci systems *Phys. Rev. B* **70** 144207
- [10] Schwalm W A and Schwalm M K 1988 Extension theory for lattice Green functions *Phys. Rev. B* **37** 9524–42
- [11] Peng R W, Huang X Q, Qiu F, Wang M, Hu A, Jiang S S and Mazzer M 2002 Symmetry-induced perfect transmission of light waves in quasiperiodic dielectric multilayers *Appl. Phys. Lett.* **80** 3063–5
- [12] Price P J 1993 Transmission and reflection peaks in ballistic transport *Appl. Phys. Lett.* **62** 289–90
- [13] Wu H-L, Goff W and Phillips P 1992 Insulator-metal transitions in random lattices containing symmetrical defects *Phys. Rev. B* **45** 1623–8
- [14] Rodrigues V, Fuhrer T and Ugarte D 2000 Signature of atomic structure in the quantum conductance of gold nanowires *Phys. Rev. Lett.* **85** 4124–7